Neural Correlates of RDoC Reward Constructs in Adolescents with Diverse Psychiatric Symptoms: A Reward Flanker Task Pilot Study

Kailyn A. L. Bradley[1], **Julia A. C. Case**[1], **Rachel D. Freed**[1], **Emily R. Stern**[1,2], and **Vilma Gabbay**[1,2,3,*]

[1]Department of Psychiatry, Icahn School of Medicine at Mount Sinai, New York, NY

[2]Department of Neuroscience, Icahn School of Medicine at Mount Sinai, New York, NY

[3]Nathan S. Kline Institute for Psychiatric Research, Orangeburg, NY

Abstract

Background—There has been growing interest under the Research Domain Criteria initiative to investigate behavioral constructs and their underlying neural circuitry. Abnormalities in reward processes are salient across psychiatric conditions and may precede future psychopathology in youth. However, the neural circuitry underlying such deficits has not been well defined. Therefore, in this pilot, we studied youth with diverse psychiatric symptoms and examined the neural underpinnings of reward anticipation, attainment, and positive prediction error (PPE, unexpected reward gain). Clinically, we focused on anhedonia, known to reflect deficits in reward function.

Methods—Twenty-two psychotropic medication-free youth, 16 with psychiatric symptoms, exhibiting a full range of anhedonia, were scanned during the Reward Flanker Task. Anhedonia severity was quantified using the Snaith-Hamilton Pleasure Scale. Functional magnetic resonance imaging analyses were false discovery rate corrected for multiple comparisons.

Results—Anticipation activated a broad network, including the medial frontal cortex and ventral striatum, while attainment activated memory and emotion-related regions such as the hippocampus and parahippocampal gyrus, but not the ventral striatum. PPE activated a right-dominant fronto-temporo-parietal network. Anhedonia was only correlated with activation of the right angular gyrus during anticipation and the left precuneus during PPE at an uncorrected threshold.

Limitations—Findings are preliminary due to the small sample size.

Conclusions—This pilot characterized the neural circuitry underlying different aspects of reward processing in youth with diverse psychiatric symptoms. These results highlight the complexity of the neural circuitry underlying reward anticipation, attainment, and PPE. Furthermore, this study underscores the importance of RDoC research in youth.

*Corresponding Author. Department of Psychiatry-1230, Icahn School of Medicine at Mount Sinai, 1 Gustave L. Levy Place, New York, NY 10029, USA, Tel.: +1 212-659-1661, Fax: +1 212-659-1693, vilma.gabbay@mssm.edu.

Introduction

The NIMH Research Domain Criteria (RDoC) initiative uses a transdiagnostic approach to identify core constructs in five functional domains that potentially contribute to psychopathology; these domains are thought to reflect common psychological and neurobiological mechanisms of dysfunction across psychiatric illnesses (Cuthbert and Insel, 2013; Insel et al., 2010). The positive valence system (PVS) is one such domain responsible for responses to pleasure and includes reward motivation, reward attainment, and reward learning (Morris and Cuthbert, 2012). The neural circuitry supporting these reward processes matures during adolescence (Paus, 2005), with this period often characterized by increased risk-taking and reward-seeking behaviors (Casey et al., 2010). Relatedly, alterations in the reward network have been associated with the early emergence of psychiatric symptoms during this sensitive period of development (Paus et al., 2008).

Anhedonia, a reduced capacity to experience pleasure, is a known prodromal symptom for various psychiatric illnesses, including depression (Dryman and Eaton, 1991) and schizophrenia (Gelber et al., 2004). Deficits in different reward processes (e.g., reward valuation, expectancy, and attainment) may result in the same anhedonic phenotype, but the neurobiological mechanisms underlying these phenomena are still largely unknown. Therefore, recent work has sought to quantify anhedonia and examine relationships between symptom severity and patterns of neural activity during reward processing. The Snaith-Hamilton Pleasure Scale (SHAPS) is one such commonly used measure of anhedonia severity and examines the capacity to experience pleasure (Snaith et al., 1995).

Functional magnetic resonance imaging (fMRI) has been widely utilized to assess reward processing (Richards et al., 2013; Urban et al., 2012). Several different task structures have been used, which may contribute to variations in fMRI findings (Richards et al., 2013). Passive reward tasks do not require active decision-making to receive probabilistically determined gains (Richards et al., 2013) and consequently may not be ideal to assess the motivation and expectancy components of reward processing. In contrast, instrumental-reward tasks do require simple action in response to a perceptual, cognitive, or motor task (Richards et al., 2013). The Monetary Incentive Delay (MID) Task is a common instrumental-reward task, in which participants respond to a simple two-choice task in order to win or lose (Knutson et al., 2000). However, reward outcomes in the MID Task are often predetermined probabilistically, and the ease of the two-choice task may not adequately impact motivation and thus performance. Building on prior work (Stern et al., 2011; Taylor et al., 2006), we developed the Reward Flanker Task (RFT) based on a combination of the common MID (Knutson et al., 2000) and Flanker (Eriksen and Eriksen, 1974) tasks, where monetary cues designate the reward value of correct responses to upcoming flanker stimuli containing a cognitive conflict component. Our approach of increasing task difficulty through the addition of a conflict component and eliminating probabilistically determined

outcomes allows for the assessment of brain function during both motivation and reward receipt processes. Importantly, we also include an unknown cue condition in the design ('?' cue instead of the monetary value) in order to allow us to additionally probe differences in neural processing of reward based on expectancy. Specifically, positive prediction error (PPE)—defined here as unexpected reward receipt—can be assessed. The study of PPE is important, as it is an interrelated facet of reward processing integral to reward learning.

In typical development, a common set of brain regions in the dopaminergic system has been associated with reward processing, including the ventral striatum (nucleus accumbens), orbitofrontal cortex (OFC), and anterior cingulate cortex (ACC) (Richards et al., 2013; Urban et al., 2012). Additional regions such as the thalamus, amygdala, insula, and inferior frontal gyrus (IFG), among others, have also been implicated in reward processing (Rademacher et al., 2010; Silverman et al., 2015). In healthy individuals, reward anticipation has been specifically associated with activity in the midbrain and ventral striatum (Knutson et al., 2001a; Knutson et al., 2001b; Knutson et al., 2005), whereas reward receipt has been associated with activity in the orbitofrontal cortex (Knutson et al., 2001a; Knutson et al., 2001b). Reward receipt has also been associated with activity in the ventral striatum, but usually during early learning and initial feedback; activation of this region switches from the reward outcome phase to the anticipatory phase during reward learning (i.e., conditioning; Galvan et al., 2005). In patient populations, alterations in ventral striatal and mesial prefrontal cortex activity during reward processing are characteristic of adult (Arrondo et al., 2015; Zhang et al., 2013) and pediatric depression (Forbes et al., 2006; Forbes and Dahl, 2012; Forbes et al., 2009; Forbes et al., 2010), as well as adult schizophrenia (Arrondo et al., 2015) and obsessive-compulsive disorder (Figee et al., 2011).

Given that striatal and mesial prefrontal cortex dysfunction during reward processing cut across psychiatric diagnostic categories, it is important to further investigate and isolate reward circuitry dysfunctions that may underlie alterations in specific phases of reward processing, including motivation, expectancy, and the experience of reward. It is particularly important to examine expectancy in reward processing because studies have shown that disruption in processing prediction errors could lead to anhedonia through disruptions in reward learning and the blunting of reward responses (Gradin et al., 2011; Greenberg et al., 2015; Kumar et al., 2008). Prediction errors occur when the expected reward outcome does not match the actual outcome, which is essential to reward learning. Gradin et al. (2011) found that both patients with depression and those with schizophrenia exhibited disruptions in neural activation in response to prediction errors; specifically, individuals with depression showed reduced activation in the striatum and midbrain that was correlated with increased anhedonia severity. In healthy individuals, but not depressed patients, there is evidence of an inverse relationship between reward expectancy and activation of the ventral striatum when processing prediction errors (Chase et al., 2013; Greenberg et al., 2015). Similarly, the recent EMBARC study found that greater anhedonia severity was associated with a reduction in this inverse relationship between reward expectancy and ventral striatal activity in response to prediction errors (Greenberg et al., 2015). Together, these studies suggest that dysfunctional prediction error processing is specifically associated with anhedonia.

Building upon the above investigations, the current study used a transdiagnostic RDoC approach to map the neurocircuitry of distinct reward processes. In this pilot investigation, we used the RFT, which allows for the discrimination of the core constructs of valuation and motivation (i.e., reward anticipation) and initial responsiveness to reward attainment (i.e. reward receipt). In addition, the RFT is able to examine brain function related to expectancy, specifically PPE. Consistent with RDoC principles, we piloted this reward task on youth with diverse mood and anxiety disorders, as well as healthy controls, in order to examine a wide range of anhedonia severity and thus reward dysfunction. We hypothesized that reward anticipation would be associated with activity in the ventral striatum, while reward attainment would evoke a broader network involving the orbitofrontal cortex and emotion-mediated limbic system. Furthermore, as PPE involves complex reward processes involved in reward learning, we expected that both anticipatory and consummatory networks would be engaged, including the ventral striatum (Chase et al., 2013; Greenberg et al., 2015). We also explored relationships between anhedonia severity as measured by the SHAPS and reward processing. We predicted that anhedonia severity would be inversely related to ventral striatal activation during reward anticipation and in response to positive prediction errors.

Methods

Participants

The sample consisted of 22 youth (M age = 16.30, SD = 2.32, range: 12–20 years; 10 females). Participants with diverse psychiatric symptoms (n = 16), regardless of whether diagnostic criteria from the Diagnostic and Statistical Manual of Mental Disorders, 4th edition (DSM-IV) were met, were recruited, along with healthy controls (HC; n = 6) with no significant presentation of psychiatric symptomatology or history of mental illness. Ten additional adolescents were scanned but excluded from all analyses: 3 for excessive head motion, 6 for poor/incomplete image acquisition, and 1 for an incidental finding on the MRI scan. Adolescents were recruited from the Mount Sinai Child and Adolescent Psychiatry Outpatient Clinic, physician referrals, and advertisements in the community. An Institutional Review Board (IRB) approved the study, and written informed consent was obtained from participants age 18 and older; those under age 18 provided signed assent, and a parent or legal guardian provided signed informed consent.

Inclusion and Exclusion Criteria

All participants were between the ages of 12 and 20 years old and did not present with any medical or neurological conditions. General exclusionary criteria included a low IQ (< 80) as assessed by the Kaufman Brief Intelligence Test [KBIT; (Kaufman, A. S. and Kaufman, 1990)], MRI contraindications, a positive drug toxicology test, and a positive pregnancy test in females.

In participants with psychiatric symptoms, current psychosis, pervasive developmental disorder, and substance abuse disorders were exclusionary. All participants were free of psychotropic or neuro-active medications for 1–3 months, depending on drug half-life.

Clinical Assessments

Even though DSM diagnoses were not used to separate participants into diagnostic categories, the Schedule for Affective Disorders and Schizophrenia for School-Age Children–Present and Lifetime Version [KSADS-PL; (Kaufman, J. et al., 1997)] was administered to the participant—as well as a parent when the participant was under age 18 years—to assess psychiatric symptomatology and exclusionary criteria. A board-certified child/adolescent psychiatrist or a licensed clinical psychologist trained in administering the KSADS carried out the diagnostic evaluation, with the final clinical report discussed between the Primary Investigator (a licensed child/adolescent psychiatrist) and the assessor. Depression severity was assessed using the clinician-rated Children's Depression Rating Scale-Revised [CDRS-R; (Poznanski et al., 1985)]. Anhedonia was quantified according to the Snaith-Hamilton Pleasure Scale [SHAPS; (Snaith et al., 1995)], which evaluates the experience of pleasure. We chose the SHAPS to assess anhedonia severity because it is one of the most widely used measures of anhedonia in clinical depression research (De Berardis et al., 2013; Farabaugh et al., 2015; Wang et al., 2015). The Chronbach's alpha for the 14 items on the SHAPS in the current sample was .897, demonstrating the high reliability of this measure.

Reward Flanker Task

During the RFT, participants made button presses and earned a reward if they correctly identified a target letter surrounded by four flanker letters (Figure 1). During each trial, a monetary cue was presented for 4–6 s, jittered in 1 s intervals. Four cues were used: low reward ("10¢"), high reward ("50¢"), no reward ("0¢"), and unknown reward ("?"). Unknown reward cues ("?") led to high ("50¢"), low ("10¢"), and no rewards ("0¢") in equal numbers and were used to examine unexpected outcomes, specifically PPE. After the cue, the flanker stimuli were presented for 300 ms, followed by a response interval that was calculated for each participant based on performance during a practice session; the mean response time during practice was multiplied by 1.5, with a maximum of 1700 ms allowed for the response interval. Participants then received feedback for 2 s informing them of the value of the obtained or unobtained reward. An inter-trial interval (ITI) between 4 and 6 s, jittered in 1 s intervals, followed the feedback interval. A total of 120 trials were presented in a pseudo-random event-related design over 4 runs, with 30 trials per run. In total, there were 30 trials each of high, low, no reward, and unknown rewards. After each run, participants were told how much money they had earned. All money was real and tallied to create a bonus given to participants at the end of the experimental session. Participants were informed of this performance-based bonus prior to completing the task in order to increase motivation.

Importantly, right before the MRI scanning session, all participants completed a RFT training session in a mock scanner in order to reduce the impact of the learning process. During this training session, participants were introduced to the rules of the RFT and learned which buttons to press in response to the stimuli by reading instructions and viewing examples. Then participants completed one full run of the RFT, comprised of 30 trials, with the same distribution of high, low, no reward, and unknown reward trials as the real MRI scanner task.

MRI Acquisition

Imaging data were acquired at Mount Sinai's Brain Imaging Center on a 3T Skyra scanner with a 16+4 head-neck coil. High resolution T1-weighted anatomical images were acquired using a magnetization prepared rapid acquisition gradient echo sequence with the following parameters: TR = 2400 ms, TE = 2.06 ms, flip angle = 8°, FOV = 256 mm×256 mm, 224 sagittal slices 0.9 mm thick, in-plane resolution = 0.9 mm×0.9 mm. Functional T2*-weighted gradient echo multiband echo planar images were acquired over 4 runs with alternating phase-encoding directions (i.e., LR, RL, LR, RL) and the following parameters: TR = 1000 ms, TE = 31.4 ms, flip angle = 60°, FOV = 624 mm × 720 mm, 374 transverse slices 2.3 mm thick, in-plane resolution = 2.3 mm × 2.3 mm. Additionally, two field maps with opposite phase-encoding directions (i.e., RL and LR) were also acquired with the following parameters: TR = 6150 ms, TE = 57 ms, flip angle = 80°, FOV = 624 mm × 720 mm, 2 transverse slices 2.3 mm thick, in-plane resolution = 2.3 mm × 2.3 mm.

MRI Data Analysis

Neuroimaging analyses were conducted using a combination of Human Connectome Project (HCP) minimal-preprocessing scripts (Glasser et al., 2013) and Statistical Parametric Mapping (SPM) version 12 (Wellcome Trust Centre for Neuroimaging, London, UK) running on a Matlab, version 2015a, platform (The MathWorks, Inc., Natick, MA, USA). Neuroimaging pre-processing included gradient non-linearity and echo planar image distortion correction (HCP), motion correction (SPM), coregistration of the functional images to the anatomical images (SPM), normalization to standard Montreal Neurological Institute (MNI) space (SPM), and spatial smoothing with a 6 mm full width at half maximum (FWHM) Gaussian kernel (SPM). Motion plots were examined, and runs with greater than 4 mm of translation or 4 degrees in rotation were eliminated from further analyses. Five participants had one run of data dropped from all analyses due to excessive motion. Three additional subjects had multiple runs with excessive motion and were therefore completely dropped from all analyses due to an inadequate number of trials for analysis.

At the first-level (subject-level), 11 task-based regressors were specified: reward anticipation (high, low, no reward, and unknown reward cues), reward attainment (high, low, and no reward feedback on correct trials, separately for known and unknown cues), and error feedback (incorrect trials). Six additional regressors of no interest modeled motion parameters from preprocessing. Each regressor was convolved with the canonical hemodynamic response function using the general linear model. First-level contrasts examined anticipation (unknown '?' and known 0¢, 10¢, 50¢ cues) and feedback (reward outcomes of 0¢, 10¢, and 50¢ with known and unknown '?' cues) conditions versus an implicit baseline. At the second-level, one-sample t-tests included age as a covariate and examined group-level whole-brain activation for contrasts of interest. Contrasts that pertained to our primary hypotheses included: reward anticipation (10¢ + 50¢ cues) vs. reward attainment (feedback from correct trials worth 10¢ + 50¢); reward attainment vs. reward anticipation; and positive prediction error [unexpected reward attainment (correct trials worth 10¢ + 50¢ that had an unknown '?' cue) vs. expected reward attainment (correct trials worth 10¢ + 50¢ that had known cues)]. We additionally explored other contrasts that

compared reward magnitude, including: reward anticipation (10¢ + 50¢ cues) vs. no reward anticipation (0¢ cues); high reward anticipation (50¢ cues) vs. low reward anticipation (10¢ cues); reward attainment (feedback from correct trials worth 10¢ + 50¢) vs. no reward attainment (feedback from correct trials worth 0¢); and high reward attainment (feedback from correct trials worth 50¢ cues) vs. low reward attainment (feedback from correct trials worth 10¢ cues).

Threshold-Free Cluster Enhancement (TFCE) as implemented in PALM (Winkler et al., 2014) was used for all second-level analyses, false discovery rate (FDR) corrected for multiple comparisons with $p < .05$. TFCE has been found to give good sensitivity compared to other methods and relies on fewer assumptions because it does not depend on selecting an initial, arbitrary cluster-forming threshold (Eklund et al., 2016; Smith and Nichols, 2009). This method specifically produces an output image based on voxel-wise values that represent the amount of cluster-like local spatial support (Smith and Nichols, 2009). Lastly, correlations between anhedonia severity (SHAPS) and brain activation during reward anticipation, attainment, and PPE were explored, controlling for age and depression severity (CDRS-R total score minus the anhedonia item); one participant did not complete that SHAPS and was therefore excluded from these analyses. Due to the exploratory nature of these analyses, a more liberal uncorrected threshold, $p < .001$ was also utilized if no results survived the conservative FDR correction.

Behavioral Data Analysis

Reaction time (RT) and accuracy (percent correct) were calculated for correct trials with a known cue value of 0¢, 10¢, and 50¢, and trials with an unknown cue, for each of the four runs of the RFT and combined. Statistical analyses were performed in SPSS, version 23. Within-subjects repeated measures ANOVA was used to assess cue-value effects on accuracy and reaction time during the RFT. Age was evaluated as a covariate; if there were significant correlations between age and either accuracy or reaction time, it was included as a covariate in an ANCOVA analysis. When assumptions of sphericity were violated, Greenhouse-Geisser corrections were used. Significance for follow-up pairwise contrasts was adjusted for multiple comparisons ($\alpha = .008 = .05/6$ comparisons: 0¢ vs. 10¢, 0¢ vs. 50¢, 0¢ vs. unknown, 10¢ vs. 50¢, 10¢ vs. unknown, and 50¢ vs. unknown). Correlations assessed associations between accuracy and reaction time on the RFT and anhedonia severity (SHAPS), controlling for depression severity (CDRS-R scores minus the anhedonia item). Spearman correlations were used, and significance was adjusted for multiple comparisons ($\alpha = .0125 = .05/4$ correlations; SHAPS and 0¢, SHAPS and 10¢, SHAPS and 50¢, and SHAPS and unknown).

Results

Demographic and Clinical Features

Data from 22 adolescents are presented. Sixteen adolescents manifested psychiatric symptoms, ten of whom met full or subclinical criteria for multiple DSM-IV disorders, including major depressive disorder, depressive disorder not otherwise specified (NOS), anxiety disorders (e.g., generalized anxiety disorder, social anxiety disorder, specific

phobia), oppositional defiant disorder (ODD), attention-deficit hyperactivity disorder (ADHD), and eating disorder NOS. Six adolescents had a diagnosis or subclinical presentation of a single disorder (1 major depressive disorder, 3 depressive disorder NOS, 1 bipolar disorder NOS, 1 ADHD). Six adolescents exhibited no symptoms consistent with a clinical or subclinical presentation of a disorder and had no history of mental illness. Demographic and clinical characteristics are presented in Table 1.

RFT Mock Scanner Training Session

Overall accuracy on the RFT training session prior to the fMRI scan was 85.00% (SD = 15.93). Less than 1% of trials were omitted [$M\% \pm SD$; 0.76 ± 1.76]. Average reaction time on the training task was 1016.14ms (SD = 267.86).

RFT Accuracy During fMRI Scan

Age was not correlated with accuracy [0¢: $\rho = -.24$, $p = .29$; 10¢: $\rho = .16$, $p = .48$; 50¢: $\rho = -.01$, $p = .96$; unknown value: $\rho = -.35$, $p = .11$] and thus not included as a covariate in the ANOVA model. There was a significant ($p < .05$) difference in accuracy (percent correct) between cue-types [$M\% \pm SD$; 0¢: 82.05 ± 16.64; 10¢: 86.44 ± 8.27; 50¢: 88.41 ± 12.32; unknown value: 86.87 ± 11.27; $F(2.06, 43.17) = 3.92$, $p = 0.03$, effect size: $\eta_p^2 = 0.16$]. Follow-up pairwise comparisons showed a significant ($p < .008$) increase in accuracy of 6.36% from trials worth 0¢ to 50¢ (99.2% CI, 1.39 to 11.34), $p = .001$. Accuracy trended towards increasing on trials worth an unknown value compared to those worth 0¢, but this difference only approached significance (99.2% CI, −.36 to 10.01), $p = .01$. No other comparisons (i.e., 0¢ vs. 10¢, 10¢ vs. 50¢, 10¢ vs. unknown, and 50¢ vs. unknown) were significant (all $ps > .008$).

The SHAPS, was not correlated with accuracy [0¢: $\rho = -.32$, $p = .17$; 10¢: $\rho = -.06$, $p = .79$; 50¢: $\rho = -.38$, $p = .09$; unknown value: $\rho = -.17$, $p = .46$].

RFT Reaction Time During fMRI Scan

Age was not correlated with reaction time [0¢: r = −.18, $p = .42$; 10¢: r = −.08, $p = .72$; 50¢: r = −.08, $p = .73$; unknown value: r = −.18, $p = .41$] and thus not included as a covariate in the ANOVA model. There were no significant differences in reaction time between cue-types [M(ms) $\pm SD$; 0¢: 980.53 ± 158.40; 10¢: 959.95 ± 159.37; 50¢: 978.17 ± 146.89; unknown value: 976.31 ± 152.22; incorrect trials: 1019.12 ± 223.39; $F(2.28, 47.79) = 1.99$, $p = 0.143$, effect size: $\eta_p^2 = 0.09$].

The SHAPS was significantly ($p < .0125$) correlated with reaction time on high-value trials only [50¢: $\rho = -.63$, $p = .003$]. Adolescents with more severe anhedonia had faster reaction times on high-value trials, and those with low anhedonia had slower reaction times. Reaction times from trials with other cue-values were not significantly correlated with anhedonia [0¢: $\rho = -.40$, $p = .08$; 10¢: $\rho = -.36$, $p = .11$; unknown value: $\rho = -.39$, $p = .09$].

Neural Activation During Reward Processing

Reward anticipation—In the contrast of reward anticipation (10¢ and 50¢) versus an implicit baseline, a large bilateral network was activated, including the posterior medial

frontal gyrus, ACC, midcingulate cortex (MCC), and posterior cingulate cortex (PCC; Table 2). Additionally, the bilateral striatum (caudate and putamen), including the ventral striatum (nucleus accumbens), thalamus, inferior and middle occipital lobe, fusiform gyrus, lingual gyrus, superior parietal lobule, insula, inferior frontal gyrus (IFG), hippocampus, and cerebellum were activated (Table 2).

In the contrast of reward anticipation (10¢ + 50¢) versus no reward anticipation (0¢), a similar broad bilateral network was activated (Supplementary Table 1). High reward anticipation versus low reward anticipation also produced this similar pattern of activation, including ventral striatal activity (Supplementary Table 1).

Reward attainment—Activation during the processing of reward attainment (i.e., correct trials worth 10¢ and 50¢ > implicit baseline) partially overlapped with that of anticipation, described above. Similar sections of the bilateral cerebellum, occipital lobe, thalamus, and dorsal striatum were activated, as well as the ACC, IFG, and hippocampus. However, there was variation in these regions, which can be seen in direct comparisons of the two conditions below. Notably, reward attainment did not activate the ventral striatum or the prominent medial frontal clusters (Figure 2).

Neural activation patterns related to the magnitude of reward feedback were also assessed. No brain regions survived the permutation testing analyses, FDR corrected, in the comparison of reward attainment (10¢ and 50¢) to no reward attainment (0¢). However, no reward attainment (0¢) compared to attainment of rewards worth 10¢ and 50¢ activated a large network, including the bilateral cerebellum posterior lobe, lingual gyrus, ACC, MCC, PCC, superior medial frontal gyrus, striatum (caudate and putamen but NOT the ventral striatum), hippocampus, middle and superior temporal gyrus, inferior and superior parietal lobules, and the fusiform gyrus (Supplementary Table 1). There were no significant differences between high- and low-value rewards.

Reward anticipation vs. attainment—While the activation maps of reward anticipation and attainment partially overlapped when each condition was compared to an implicit baseline, as described above, in the direct comparison of these phases (i.e., reward anticipation on trials worth 10¢ and 50¢ > reward attainment on correct trials worth 10¢ and 50¢), there were several prominent distinctions. A large cluster in the bilateral posterior medial frontal gyrus, ACC, MCC, and precuneus distinguished anticipation from attainment (Table 2, Figure 2). Additionally, the ventral striatum (nucleus accumbens) was only activated during reward anticipation (Figure 2). Activation of the striatum, particularly the caudate, was more robust and distributed in reward anticipation and more restricted and dorsal in reward attainment (Figure 2). Moreover, the bilateral thalamus and insula were more strongly activated during anticipation. Conversely, fewer regions were more strongly activated during reward attainment. The bilateral lingual gyrus, fusiform gyrus, cuneus, parahippocampal gyrus, hippocampus, and dorsal caudate were more strongly activated during reward attainment (Table 2, Figure 2).

Positive prediction error—PPE was assessed through the comparison of unexpected reward attainment (i.e., trials with unknown cues that resulted in a 10¢ or 50¢ reward) to

expected reward attainment (i.e., trials with known cues that resulted in a 10¢ or 50¢ reward). PPE resulted in activation of a very large bilateral, but right-dominant, fronto-temporo-parietal network, including the ventral striatum, detailed in Table 2 and Figure 3. Many of the same anterior and posterior medial frontal regions activated during reward anticipation were activated during PPE, as well as the occipital, limbic, and memory-related regions from reward attainment. However, there was additional robust activation of the bilateral (but right dominant) inferior, middle, and superior temporal lobes. Additionally, activity in the striatum also extended into the ventral striatum (nucleus accumbens).

Correlations between reward processing and anhedonia—The SHAPS was not related to activity during reward anticipation or attainment when TFCE analyses were FDR corrected for multiple comparisons with $p < .05$. However, when analyses were explored at a much more liberal threshold, with $p < .001$, there was a positive correlation between activation of the right angular gyrus during reward anticipation and anhedonia severity (Table 3). Additionally, there was a small positive correlation between activation of the left precuneus in response to PPEs and anhedonia severity (Table 3).

Discussion

This pilot study examined behavior and brain functioning using the Reward Flanker Task, which allows the mapping of the neural circuitry underlying several distinct and interrelated reward processes—reward anticipation, PPE, and attainment—in adolescents with diverse psychiatric symptoms and those with no significant symptomatology. In the direct comparison of reward phases, anticipation resulted in recruitment of a large network, most prominently distinguished by activation of the bilateral posterior medial frontal gyrus, ACC, MCC, precuneus, and right ventral striatum. Conversely, activation during reward attainment overlapped, but did not include, the posterior medial frontal gyrus or ventral striatal clusters, and instead, more strongly activated the bilateral lingual gyrus, cuneus, parahippocampal gyrus, and hippocampus. Expectancy also played a role in reward network activation, with PPE, or unexpected reward receipt, activating a bilateral but right-dominant fronto-temporo-parietal network that also included the ventral striatum. Lastly, anhedonia severity was not related to activation during reward processing when results were FDR corrected for multiple comparisons due to the small sample size. However, when viewed at a more liberal threshold, there was a modest relationship between activity in the right angular gyrus during reward anticipation and anhedonia severity and between the left precuneus and anhedonia in response to PPEs. With regard to behavioral performance, there were no differences in reaction time based on trial value across all adolescents, but individuals that had lower anhedonia severity responded slower on high-value trials (50¢). Additionally, adolescents were more accurate on high-value trials (50¢) than those worth no reward (0¢), but accuracy was not associated with anhedonia severity.

Reward Anticipation, Attainment, and Positive Prediction Error

While we found that neural recruitment in both the anticipation and attainment phases of reward processing partially overlapped, there were also notable distinctions. Anticipation was most prominently associated with activation of the posterior medial frontal gyrus, ACC,

MCC, precuneus, and ventral striatum, when compared to reward attainment. Consistent with these findings, the ventral striatum is characteristically activated during reward appraisal and anticipation in healthy (Knutson et al., 2001a; Knutson et al., 2001b; Rademacher et al., 2010) and psychiatric populations, including euthymic adults with bipolar disorder (Nusslock et al., 2012), and adolescents (Forbes and Dahl, 2012) and adults with depression (Zhang et al., 2013). This finding is also consistent with Galvan et al.'s (2005) study that showed ventral striatal activation shifts to the anticipatory phase after learning takes place, which is consistent with our task design since participants underwent a training session prior to the fMRI scan. Moreover, ascending dopaminergic projections from the ventral tegmental area are associated with reward assessment and appraisal in animal and human models (Knutson et al., 2003) and target the striatal, limbic, and paralimbic regions (Knutson et al., 2000). Increased firing of dopaminergic neurons has been shown to enhance the BOLD signal in these regions (Marota et al., 2000). Therefore, increased dopamine release in response to anticipation of monetary reward may result in activation of the ventral striatum during reward valuation and anticipation. Furthermore, the mesial prefrontal cortex and ACC have outputs to the supplementary motor area and hypothalamus, which may be involved in coordinating responses to incentives (Knutson et al., 2000). Thus, the greater activation of the posterior medial frontal cortex, ACC, and MCC during reward anticipation may facilitate the conflict resolution and motor processes associated with responses to flanker stimuli in the RFT.

Conversely, when compared to reward anticipation, attainment did not result in activation of the medial frontal and ventral striatal clusters (Figure 2). Instead, regions related to memory and emotional processing were more strongly activated during reward attainment, such as the bilateral parahippocampal gyrus, hippocampus, fusiform gyrus, lingual gyrus, and cuneus. Support of these findings in the literature is less unanimous. For example, receipt of a reward has been characterized by activation of the mesial prefrontal cortex, while anticipation activates the ventral striatum (Knutson et al., 2003). We found both of these regions activated more in the anticipatory phase. Moreover, the reward feedback period is often associated with activity in the orbitofrontal cortex (OFC) in typically developing individuals (Knutson et al., 2001b). We found modest activation of the right orbitofrontal cortex during reward attainment, and bilateral activation of this region during reward anticipation. Additionally, activation differences in the prefrontal cortex between our study and others may be related to two key differences in task design. First, in the RFT, participants must actively resolve conflict of the flanker stimuli in order to make the correct response. Cognitive control and conflict processing are elicited by the traditional Flanker Task, with the ACC strongly activated in response to these processes (Kennerley et al., 2006). The commonly used MID Task still requires an active button press, but the two-choice task is usually less cognitively demanding and does not involve conflict resolution. The ACC may thus be recruited in the anticipatory phase during the RFT to help process the more challenging upcoming flanker stimuli. Second, task timing may influence the neural signals that are picked up from different phases of reward processing. For example, previous work has found little difference between striatal and mesial prefrontal cortex activation during the reward anticipation and attainment phases (Breiter et al., 2001), which Knutson et al. (2003) attributed to variations in timing between reward phases in different task designs.

Expectancy also influenced reward network activation. Specifically, PPE was assessed through the comparison of unexpected reward outcomes to expected reward outcomes. PPE resulted in the activation of a bilateral but right-dominant fronto-temporo-parietal network. There is evidence from animal models that neurons in the dopaminergic system, specifically in the caudate and lateral prefrontal cortex, respond to both positive and negative prediction errors (Asaad and Eskandar, 2011; Rohe et al., 2012). Additional investigations found the ACC was activated in response to PPE (Vassena et al., 2014), while the striatum was more generally associated with both positive and negative unexpected outcomes (Rohe et al., 2012; Tricomi et al., 2004). In the current study, while the ACC was not activated in response to expected reward attainment, it was activated, along with the caudate, putamen, and ventral striatum, in response to unexpected reward attainment (i.e., PPE). This difference is not surprising given the role of the ACC and striatum in cognitive control, reappraisal, and salience detection (Kennerley et al., 2006; Seeley et al., 2007). The unexpected outcome was salient and may have resulted in greater re-appraisal of the rewarding outcome.

Relationships Between Anhedonia Measures and Reward Circuitry

Contrary to our hypothesis, the SHAPS, a measure of self-reported consummatory anhedonia, was not related to neural activation during reward anticipation or attainment when fMRI results were FDR corrected for multiple comparisons using permutation testing, with $p < .05$. This result is not surprising given the small sample size of the correlational analyses (n = 21). In order to explore the potential association between anhedonia severity and alterations in neural activation, the results of TFCE analyses were viewed using a more liberal uncorrected threshold, with $p < .001$. At this very liberal threshold, there was a potential association between activation of the inferior parietal lobule, specifically the right angular gyrus, during reward anticipation and increased anhedonia severity. Adolescents with increased anhedonia recruited this region, which is commonly associated with visual-spatial attention toward salient features and is frequently involved in memory retrieval (Seghier, 2013). Additionally, activation of the left precuneus was mildly correlated with PPE. Our original hypothesis that ventral striatal activity during reward processing, specifically PPE, would be correlated with anhedonia severity was not supported here. However, these results do suggest that there may be some relationship between anhedonia severity and reward processing. Given the exploratory, preliminary nature of these findings, this is merely speculative until further investigation of the association between dimensional measures of anhedonia severity and neural activation during reward processing can be replicated in larger samples.

Behavioral Performance on the RFT

There was a significant difference in accuracy based on monetary incentive; adolescents were more accurate on high-value trials (50¢) compared to those worth no reward (0¢). However, there were no differences in accuracy between high- and low-value (10¢) trials. Additionally, there were no differences in reaction time based on trial value. This finding is only partially consistent with studies of monetary or social rewards in adolescents, which typically show an increase in accuracy on higher value trials (Demurie et al., 2012). Moreover, previous studies in adolescents (Demurie et al., 2012) and adults (Rademacher et

al., 2010; Spreckelmeyer et al., 2009; Stern et al., 2011) have also shown that reaction times become faster with increasing reward intensity. Our lack of accuracy and reaction time differences may suggest that a larger monetary discrepancy between high- and low-value trials is necessary to differentially motivate such a heterogeneous population of adolescents. However, it is also possible that social rewards may differentially motivate adolescents. These issues require additional investigation.

While there were few differences in behavioral performance based on monetary incentive alone, there was a correlation between reaction time and anhedonia severity. Adolescents that had higher anhedonia severity responded quicker on high-value trials, while those that had lower anhedonia severity responded slower. However, there was no association between anhedonia and accuracy. It is possible that adolescents with greater anhedonia may not place as much importance on high-value 50¢ reward targets since reward valuation and learning might be blunted in this population (Kumar et al., 2008), and thus they are quicker to respond due to indifference. The literature suggests that individuals with greater anhedonia may require a higher threshold of reward stimulation to experience pleasureable effects of reward (Leventhal et al., 2014; Schlaepfer et al., 2008; Wise, 2008). Alternately, adolescents with lower anhedonia may find 50¢ rewards to be more potent reinforcers and thus take a little longer to respond to ensure accuracy.

Limitations

There are several limitations to the current study. First, as this was a pilot investigation, low power from the small sample size may limit the interpretation of our conclusions, especially with regard to the correlations with anhedonia severity. Even though our primary fMRI results report effects that are corrected for multiple comparisons using permutation testing, these findings should be considered preliminary. Additionally, since calculation of the reward anticipation condition did not exclude incorrect or omitted trials but the reward attainment condition did, inattention could potentially account for some of the observed differences between the two conditions. For example, studies have found associations between inattention and the cuneus, precuneus, and temporo-occipital circuits (Lei et al., 2014), particularly in ADHD samples, a co-morbid diagnosis also present in some of our participants. Therefore, it is possible that activation of these regions in the anticipation vs. attainment contrast could be due to inattention. Overall, accuracy rates were very high across the group, but this should still be considered when interpreting the findings. Furthermore, the lack of robust differences in accuracy and reaction time on the RFT according to high (50¢) and low (10¢) monetary incentive may be due to the heterogeneity of the sample. Alternately, it is unclear if other forms of reward, such as social incentives, may better relate to adolescents' motivation and common clinical measures of anhedonia severity. This is a growing area of research, especially in adolescents, and warrants further investigation (Olino et al., 2015; Silk et al., 2014). Furthermore, the RFT does not assess negative prediction error (i.e., unexpected loss) or punishment. Neural responses to loss and punishment may be strongly related to current clinical measures of anhedonia severity, such as the SHAPS, which quantifies consummatory anhedonia.

Conclusions

Despite these limitations, the present study offers an important extension of the existing literature by using a novel reward task on a diverse sample of youth with and without psychiatric symptoms. Furthermore, we show the utility of adopting an RDoC framework to transdiagnostically assess associations between distinct neural circuitry of separable phases of reward processing and dimensional measures of psychiatric symptoms. Future studies with larger samples are needed to extend this investigation and examine discrete mechanisms of reward processing using both fMRI and EEG, which has better temporal sensitivity to separate out stages of reward processing.

Supplementary Material

Refer to Web version on PubMed Central for supplementary material.

References

Arrondo G, Segarra N, Metastasio A, Ziauddeen H, Spencer J, Reinders NR, Dudas RB, Robbins TW, Fletcher PC, Murray GK. Reduction in ventral striatal activity when anticipating a reward in depression and schizophrenia: A replicated cross-diagnostic finding. Front. Psychol. 2015; 6:1280. [PubMed: 26379600]

Asaad WF, Eskandar EN. Encoding of both positive and negative reward prediction errors by neurons of the primate lateral prefrontal cortex and caudate nucleus. J. Neurosci. 2011; 31(49):17772–17787. [PubMed: 22159094]

Breiter HC, Aharon I, Kahneman D, Dale A, Shizgal P. Functional imaging of neural responses to expectancy and experience of monetary gains and losses. Neuron. 2001; 30(2):619–639. [PubMed: 11395019]

Casey BJ, Duhoux S, Malter Cohen M. Adolescence: What do transmission, transition, and translation have to do with it? Neuron. 2010; 67(5):749–760. [PubMed: 20826307]

Chase HW, Nusslock R, Almeida JR, Forbes EE, LaBarbara EJ, Phillips ML. Dissociable patterns of abnormal frontal cortical activation during anticipation of an uncertain reward or loss in bipolar versus major depression. Bipolar Disord. 2013; 15(8):839–854. [PubMed: 24148027]

Cuthbert BN, Insel TR. Toward the future of psychiatric diagnosis: The seven pillars of rdoc. BMC Med. 2013; 11:126. [PubMed: 23672542]

De Berardis D, Marini S, Serroni N, Rapini G, Iasevoli F, Valchera A, Signorelli M, Aguglia E, Perna G, Salone A, Di Iorio G, Martinotti G, Di Giannantonio M. S-adenosyl-l-methionine augmentation in patients with stage ii treatment-resistant major depressive disorder: An open label, fixed dose, single-blind study. Scientific World J. 2013; 2013:204649.

Demurie E, Roeyers H, Baeyens D, Sonuga-Barke E. The effects of monetary and social rewards on task performance in children and adolescents: Liking is not enough. Int. J. Methods Psychiatr. Res. 2012; 21(4):301–310. [PubMed: 23148022]

Dryman A, Eaton WW. Affective symptoms associated with the onset of major depression in the community: Findings from the us national institute of mental health epidemiologic catchment area program. Acta Psychiatr. Scand. 1991; 84(1):1–5. [PubMed: 1927557]

Eklund A, Nichols TE, Knutsson H. Cluster failure: Why fmri inferences for spatial extent have inflated false-positive rates. Proc. Natl. Acad. Sci. U. S. A. 2016; 113(28):7900–7905. [PubMed: 27357684]

Eriksen BA, Eriksen CW. Effects of noise letters upon the identification of a target letter in a nonsearch task. P&P. 1974; 16(1):143–149.

Farabaugh A, Fisher L, Nyer M, Holt D, Cohen M, Baer L, Shapero BG, Huz I, Cardoos A, Fava M, Alpert JE. Similar changes in cognitions following cognitive-behavioral therapy or escitalopram

for major depressive disorder: Implications for mechanisms of change. Ann. Clin. Psychiatry. 2015; 27(2):118–126. [PubMed: 25954938]

Figee M, Vink M, de Geus F, Vulink N, Veltman DJ, Westenberg H, Denys D. Dysfunctional reward circuitry in obsessive-compulsive disorder. Biol. Psychiatry. 2011; 69(9):867–874. [PubMed: 21272861]

Forbes EE, Christopher May J, Siegle GJ, Ladouceur CD, Ryan ND, Carter CS, Birmaher B, Axelson DA, Dahl RE. Reward-related decision-making in pediatric major depressive disorder: An fmri study. J. Child Psychol. Psychiatry. 2006; 47(10):1031–1040. [PubMed: 17073982]

Forbes EE, Dahl RE. Research review: Altered reward function in adolescent depression: What, when and how? J. Child Psychol. Psychiatry. 2012; 53(1):3–15. [PubMed: 22117893]

Forbes EE, Hariri AR, Martin SL, Silk JS, Moyles DL, Fisher PM, Brown SM, Ryan ND, Birmaher B, Axelson DA, Dahl RE. Altered striatal activation predicting real-world positive affect in adolescent major depressive disorder. Am. J. Psychiatry. 2009; 166(1):64–73. [PubMed: 19047324]

Forbes EE, Ryan ND, Phillips ML, Manuck SB, Worthman CM, Moyles DL, Tarr JA, Sciarrillo SR, Dahl RE. Healthy adolescents' neural response to reward: Associations with puberty, positive affect, and depressive symptoms. J. Am. Acad. Child Adolesc. Psychiatry. 2010; 49(2):162–172. e161–e165. [PubMed: 20215938]

Galvan A, Hare TA, Davidson M, Spicer J, Glover G, Casey BJ. The role of ventral frontostriatal circuitry in reward-based learning in humans. J. Neurosci. 2005; 25(38):8650–8656. [PubMed: 16177032]

Gelber EI, Kohler CG, Bilker WB, Gur RC, Brensinger C, Siegel SJ, Gur RE. Symptom and demographic profiles in first-episode schizophrenia. Schizophr. Res. 2004; 67(2–3):185–194. [PubMed: 14984877]

Glasser MF, Sotiropoulos SN, Wilson JA, Coalson TS, Fischl B, Andersson JL, Xu J, Jbabdi S, Webster M, Polimeni JR, Van Essen DC, Jenkinson M. The minimal preprocessing pipelines for the human connectome project. NeuroImage. 2013; 80:105–124. [PubMed: 23668970]

Gradin VB, Kumar P, Waiter G, Ahearn T, Stickle C, Milders M, Reid I, Hall J, Steele JD. Expected value and prediction error abnormalities in depression and schizophrenia. Brain. 2011; 134(Pt 6): 1751–1764. [PubMed: 21482548]

Greenberg T, Chase HW, Almeida JR, Stiffler R, Zevallos CR, Aslam HA, Deckersbach T, Weyandt S, Cooper C, Toups M, Carmody T, Kurian B, Peltier S, Adams P, McInnis MG, Oquendo MA, McGrath PJ, Fava M, Weissman M, Parsey R, Trivedi MH, Phillips ML. Moderation of the relationship between reward expectancy and prediction error-related ventral striatal reactivity by anhedonia in unmedicated major depressive disorder: Findings from the embarc study. Am. J. Psychiatry. 2015; 172(9):881–891. [PubMed: 26183698]

Insel T, Cuthbert B, Garvey M, Heinssen R, Pine DS, Quinn K, Sanislow C, Wang P. Research domain criteria (rdoc): Toward a new classification framework for research on mental disorders. Am. J. Psychiatry. 2010; 167(7):748–751. [PubMed: 20595427]

Kaufman, AS., Kaufman, NL. Manual for the kaufman brief intelligence test. Circle Pines, MN: American Guidance Service; 1990.

Kaufman J, Birmaher B, Brent D, Rao U, Flynn C, Moreci P, Williamson D, Ryan N. Schedule for affective disorders and schizophrenia for school-age children-present and lifetime version (k-sads-pl): Initial reliability and validity data. J. Am. Acad. Child Adolesc. Psychiatry. 1997; 36(7):980–988. [PubMed: 9204677]

Kennerley SW, Walton ME, Behrens TE, Buckley MJ, Rushworth MF. Optimal decision making and the anterior cingulate cortex. Nat. Neurosci. 2006; 9(7):940–947. [PubMed: 16783368]

Knutson B, Adams CM, Fong GW, Hommer D. Anticipation of increasing monetary reward selectively recruits nucleus accumbens. J. Neurosci. 2001a; 21(16):Rc159. [PubMed: 11459880]

Knutson B, Fong GW, Adams CM, Varner JL, Hommer D. Dissociation reward anticipation and outcome with event-related fmri. Neuroreport. 2001b; 12(17):3683–3687. [PubMed: 11726774]

Knutson B, Fong GW, Bennett SM, Adams CM, Hommer D. A region of mesial prefrontal cortex tracks monetarily rewarding outcomes: Characterization with rapid event-related fmri. NeuroImage. 2003; 18(2):263–272. [PubMed: 12595181]

Knutson B, Taylor J, Kaufman M, Peterson R, Glover G. Distributed neural representation of expected value. J. Neurosci. 2005; 25(19):4806–4812. [PubMed: 15888656]

Knutson B, Westdorp A, Kaiser E, Hommer D. Fmri visualization of brain activity during a monetary incentive delay task. NeuroImage. 2000; 12(1):20–27. [PubMed: 10875899]

Kumar P, Waiter G, Ahearn T, Milders M, Reid I, Steele JD. Abnormal temporal difference reward-learning signals in major depression. Brain. 2008; 131(Pt 8):2084–2093. [PubMed: 18579575]

Lei D, Ma J, Du X, Shen G, Jin X, Gong Q. Microstructural abnormalities in the combined and inattentive subtypes of attention deficit hyperactivity disorder: A diffusion tensor imaging study. Sci. Rep. 2014; 4:6875. [PubMed: 25363043]

Leventhal AM, Trujillo M, Ameringer KJ, Tidey JW, Sussman S, Kahler CW. Anhedonia and the relative reward value of drug and nondrug reinforcers in cigarette smokers. J. Abnorm. Psychol. 2014; 123(2):375–386. [PubMed: 24886011]

Marota JJ, Mandeville JB, Weisskoff RM, Moskowitz MA, Rosen BR, Kosofsky BE. Cocaine activation discriminates dopaminergic projections by temporal response: An fmri study in rat. NeuroImage. 2000; 11(1):13–23. [PubMed: 10686113]

Morris SE, Cuthbert BN. Research domain criteria: Cognitive systems, neural circuits, and dimensions of behavior. Dialogues Clin. Neurosci. 2012; 14(1):29–37. [PubMed: 22577302]

Nusslock R, Almeida JR, Forbes EE, Versace A, Frank E, Labarbara EJ, Klein CR, Phillips ML. Waiting to win: Elevated striatal and orbitofrontal cortical activity during reward anticipation in euthymic bipolar disorder adults. Bipolar Disord. 2012; 14(3):249–260. [PubMed: 22548898]

Olino TM, Silk JS, Osterritter C, Forbes EE. Social reward in youth at risk for depression: A preliminary investigation of subjective and neural differences. J. Child Adolesc. Psychopharmacol. 2015; 25(9):711–721. [PubMed: 26469133]

Paus T. Mapping brain maturation and cognitive development during adolescence. Trends Cogn. Sci. 2005; 9(2):60–68. [PubMed: 15668098]

Paus T, Keshavan M, Giedd JN. Why do many psychiatric disorders emerge during adolescence? Nat. Rev. Neurosci. 2008; 9(12):947–957. [PubMed: 19002191]

Poznanski E, Freeman L, Mokros H. Children's depression rating scale-revised. Psychopharmacol. Bull. 1985; 21:979–989.

Rademacher L, Krach S, Kohls G, Irmak A, Grunder G, Spreckelmeyer KN. Dissociation of neural networks for anticipation and consumption of monetary and social rewards. NeuroImage. 2010; 49(4):3276–3285. [PubMed: 19913621]

Richards JM, Plate RC, Ernst M. A systematic review of fmri reward paradigms used in studies of adolescents vs. Adults: The impact of task design and implications for understanding neurodevelopment. Neurosci. Biobehav. Rev. 2013; 37(5):976–991. [PubMed: 23518270]

Rohe T, Weber B, Fliessbach K. Dissociation of bold responses to reward prediction errors and reward receipt by a model comparison. Eur. J. Neurosci. 2012; 36(3):2376–2382. [PubMed: 22595033]

Schlaepfer TE, Cohen MX, Frick C, Kosel M, Brodesser D, Axmacher N, Joe AY, Kreft M, Lenartz D, Sturm V. Deep brain stimulation to reward circuitry alleviates anhedonia in refractory major depression. Neuropsychopharmacology. 2008; 33(2):368–377. [PubMed: 17429407]

Seeley WW, Menon V, Schatzberg AF, Keller J, Glover GH, Kenna H, Reiss AL, Greicius MD. Dissociable intrinsic connectivity networks for salience processing and executive control. J. Neurosci. 2007; 27(9):2349–2356. [PubMed: 17329432]

Seghier ML. The angular gyrus: Multiple functions and multiple subdivisions. Neuroscientist. 2013; 19(1):43–61. [PubMed: 22547530]

Silk JS, Siegle GJ, Lee KH, Nelson EE, Stroud LR, Dahl RE. Increased neural response to peer rejection associated with adolescent depression and pubertal development. Soc. Cogn. Affect. Neurosci. 2014; 9(11):1798–1807. [PubMed: 24273075]

Silverman MH, Jedd K, Luciana M. Neural networks involved in adolescent reward processing: An activation likelihood estimation meta-analysis of functional neuroimaging studies. NeuroImage. 2015; 122:427–439. [PubMed: 26254587]

Smith SM, Nichols TE. Threshold-free cluster enhancement: Addressing problems of smoothing, threshold dependence and localisation in cluster inference. NeuroImage. 2009; 44(1):83–98. [PubMed: 18501637]

Snaith RP, Hamilton M, Morley S, Humayan A, Hargreaves D, Trigwell P. A scale for the assessment of hedonic tone the snaith-hamilton pleasure scale. Br. J. Psychiatry. 1995; 167(1):99–103. [PubMed: 7551619]

Spreckelmeyer KN, Krach S, Kohls G, Rademacher L, Irmak A, Konrad K, Kircher T, Grunder G. Anticipation of monetary and social reward differently activates mesolimbic brain structures in men and women. Soc. Cogn. Affect. Neurosci. 2009; 4(2):158–165. [PubMed: 19174537]

Stern ER, Welsh RC, Fitzgerald KD, Gehring WJ, Lister JJ, Himle JA, Abelson JL, Taylor SF. Hyperactive error responses and altered connectivity in ventromedial and frontoinsular cortices in obsessive-compulsive disorder. Biol. Psychiatry. 2011; 69(6):583–591. [PubMed: 21144497]

Taylor SF, Martis B, Fitzgerald KD, Welsh RC, Abelson JL, Liberzon I, Himle JA, Gehring WJ. Medial frontal cortex activity and loss-related responses to errors. J. Neurosci. 2006; 26(15):4063–4070. [PubMed: 16611823]

Tricomi EM, Delgado MR, Fiez JA. Modulation of caudate activity by action contingency. Neuron. 2004; 41(2):281–292. [PubMed: 14741108]

Urban NB, Slifstein M, Meda S, Xu X, Ayoub R, Medina O, Pearlson GD, Krystal JH, Abi-Dargham A. Imaging human reward processing with positron emission tomography and functional magnetic resonance imaging. Psychopharmacology (Berl.). 2012; 221(1):67–77. [PubMed: 22052081]

Vassena E, Krebs RM, Silvetti M, Fias W, Verguts T. Dissociating contributions of acc and vmpfc in reward prediction, outcome, and choice. Neuropsychologia. 2014; 59:112–123. [PubMed: 24813149]

Wang S, Qian M, Zhong H, Song G, Lu M, Feng R, Zhang L, Ni J, Chen W. Comparison of the effectiveness of duloxetine in depressed patients with and without a family history of affective disorders in first-degree relatives. Shanghai Arch. Psychiatry. 2015; 27(4):237–245. [PubMed: 26549960]

Winkler AM, Ridgway GR, Webster MA, Smith SM, Nichols TE. Permutation inference for the general linear model. NeuroImage. 2014; 92:381–397. [PubMed: 24530839]

Wise RA. Dopamine and reward: The anhedonia hypothesis 30 years on. Neurotox. Res. 2008; 14(2–3):169–183. [PubMed: 19073424]

Zhang WN, Chang SH, Guo LY, Zhang KL, Wang J. The neural correlates of reward-related processing in major depressive disorder: A meta-analysis of functional magnetic resonance imaging studies. J. Affect. Disord. 2013; 151(2):531–539. [PubMed: 23856280]

Highlights

- Reward anticipation activates medial prefrontal and ventral striatal regions

- Reward attainment activates memory and emotion-related regions

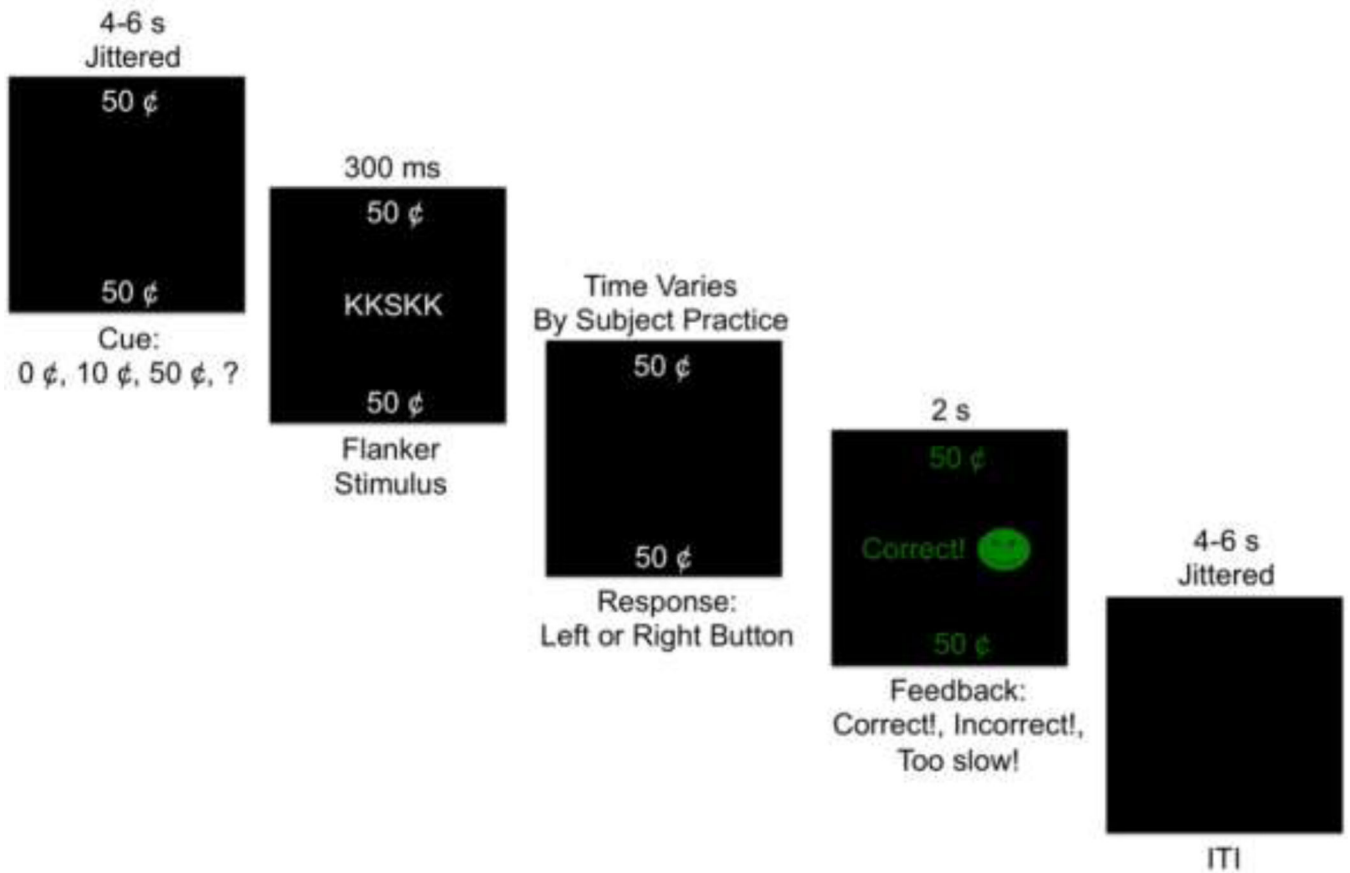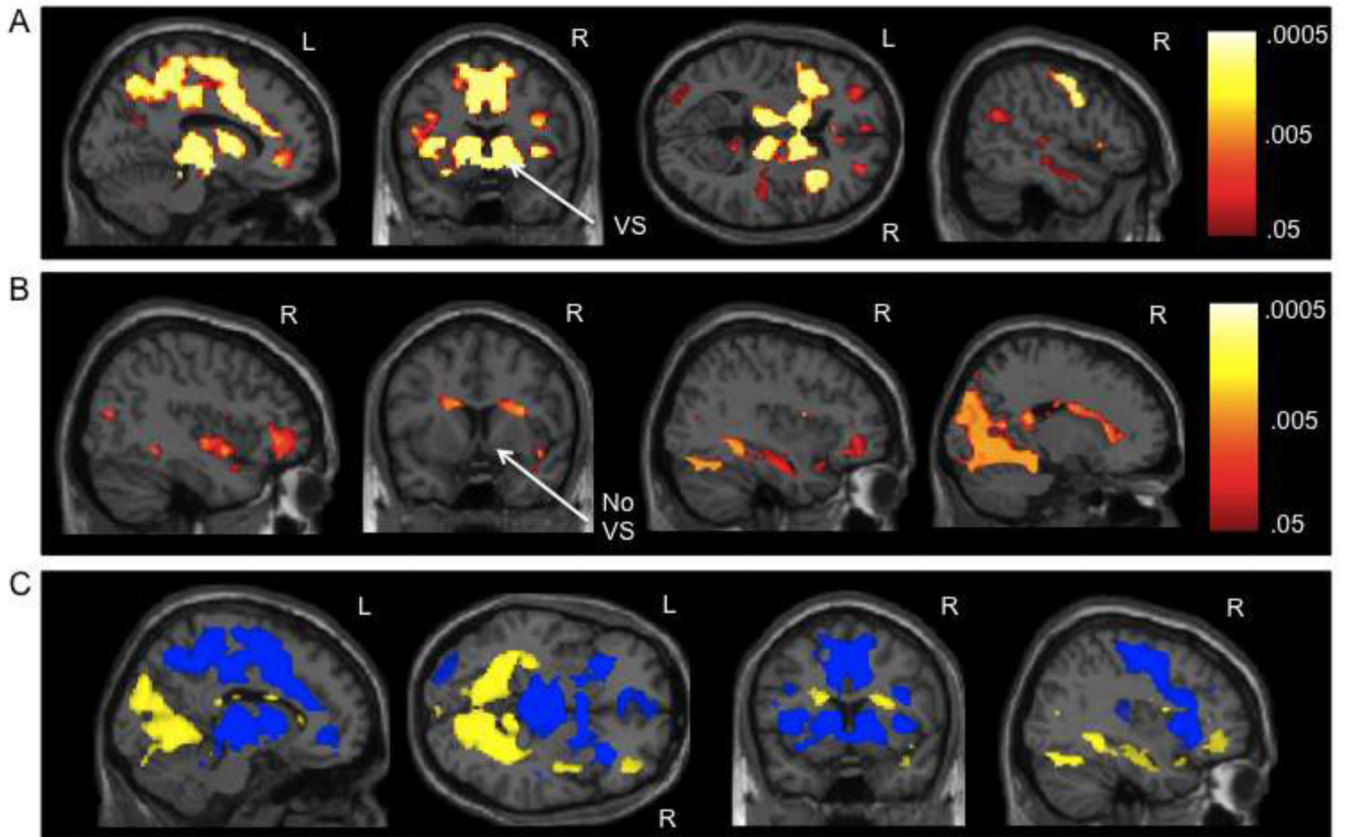- Anhedonia is modestly correlated with neural activation during reward processing

Figure 1.
Reward Flanker Task (RFT). Depiction of an example trial on the RFT.
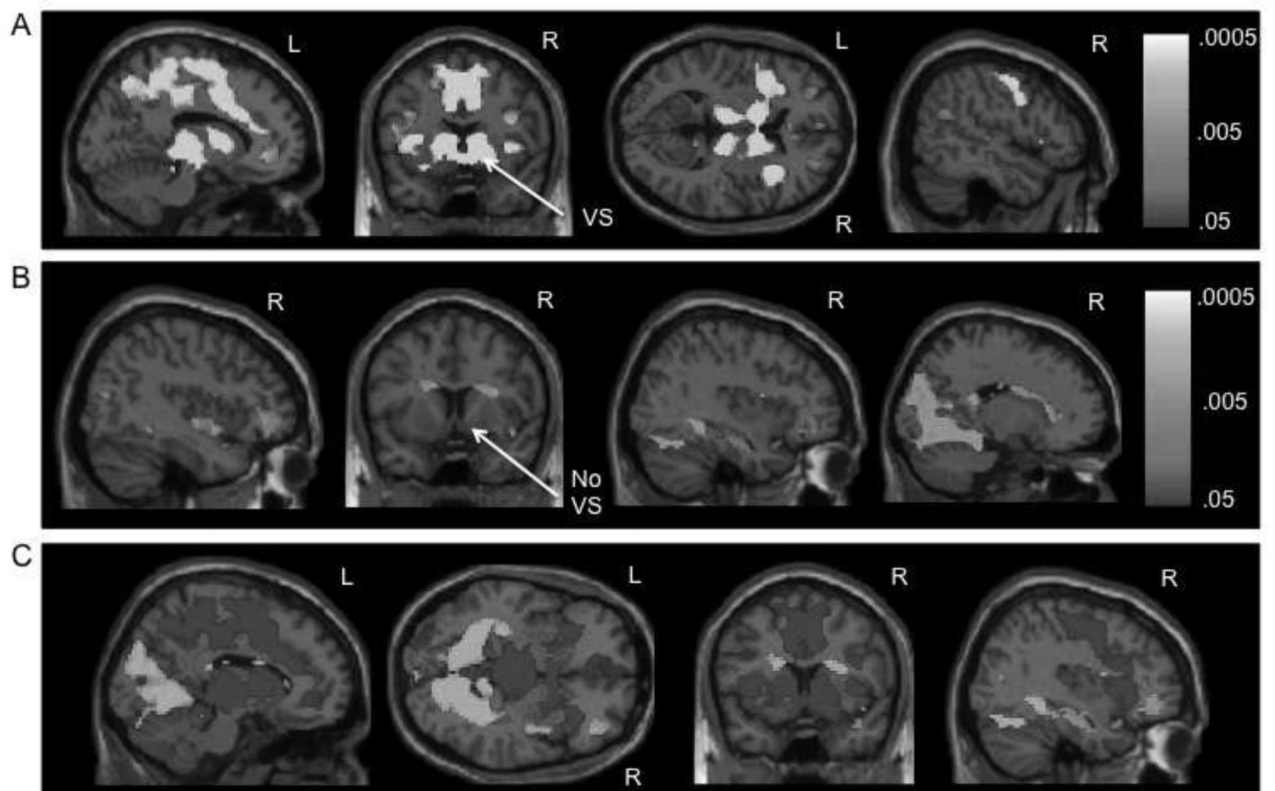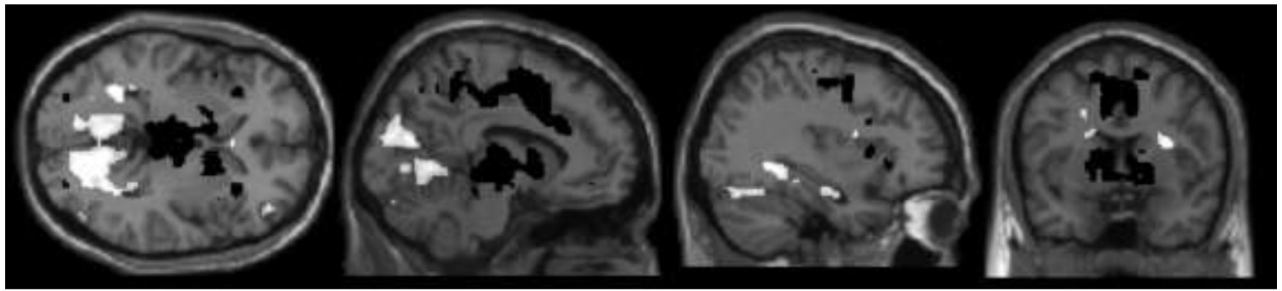
Figure 2.
A) Neural activation during reward anticipation vs. reward attainment. B) Neural activation during reward attainment vs. reward anticipation. For 2A and 2B, *p*-value maps from the permutation testing with threshold-free cluster enhancement analyses are presented; *p*-values are false discovery rate (FDR) corrected for multiple comparisons (*p* < .05). C) Depiction of the *p*-value maps from 2A and 2B overlaid on one another to show differences between the contrasts, with blue (dark gray) = reward anticipation vs. reward attainment and yellow (light gray) = reward attainment vs. reward anticipation. VS = ventral striatum
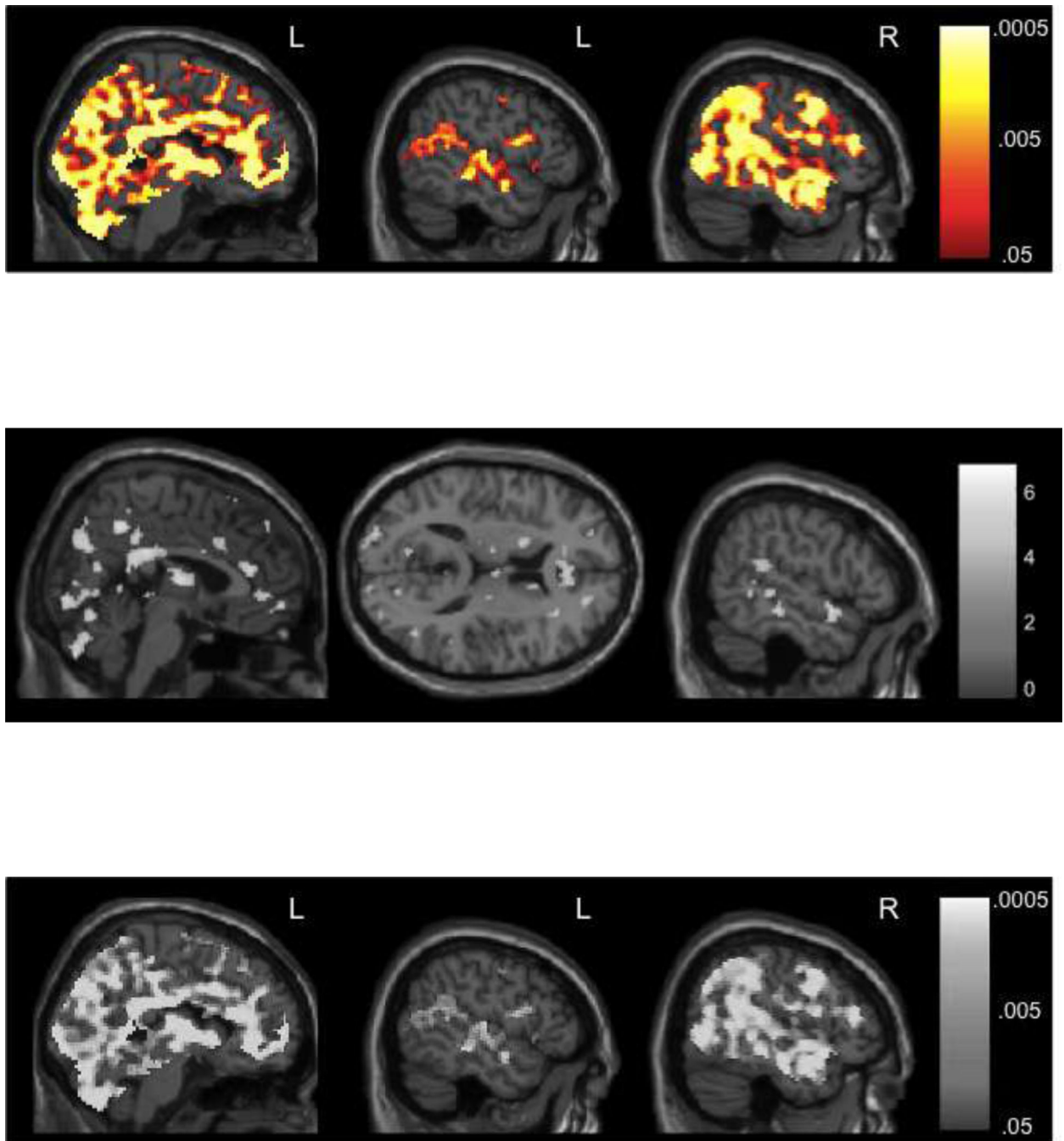
Figure 3.
Neural activation during positive prediction error (PPE). PPE was defined as unexpected reward attainment (correct feedback from trials with an unknown cue '?' worth 10¢ and 50¢) vs. expected reward attainment (correct feedback from trials with a known cue worth 10¢ and 50¢). Images depict p-value maps from the permutation testing with threshold-free cluster enhancement analyses; p-values are false discovery rate (FDR) corrected for multiple comparisons ($p < .05$).

Table 1

Demographic and Clinical Characteristics

Demographics	Total Sample ($N = 22$)
Age [$M \pm SD$] (Range)	16.30 ± 2.32 (12–20)
Gender [n Female/Male] (%)	10/12 (45.50/54.50)
Ethnicity [n Caucasian/African American/ Hispanic/Other] (%)	3/9/6/4 (13.64/40.91/27.27/18.18)
Psychiatric Profile [n] (%)	
Major Depressive Disorder (MDD)	8 (36.36)
Depressive Disorder Not Otherwise Specified (DDNOS)	4 (18.18)
Bipolar Disorder Not Otherwise Specified (BDNOS)	1 (4.55)
Anxiety Disorders (e.g., Generalized, Social, Phobia)	7 (31.82)
Oppositional Defiant Disorder (ODD)	3 (13.64)
Attention-deficit Hyperactivity Disorder (ADHD)	5 (22.73)
Eating Disorder	1 (4.55)
None (No History of Psychiatric Illness)	6 (27.27)
Clinical Assessments [$M \pm SD$] (Range)	
Med-naïve/Med-free/Medicated [n] (%)	18/4/0 (81.82/18.18/0)
CDRS-R[a]	36.41 ± 17.89 (17–78)
CDRS-R Minus Anhedonia	33.86 ± 16.20 (16–72)
SHAPS[b*]	22.67 ± 7.05 (14–38)

Note.

[a] Children's Depression Rating Scale-Revised;

[b] Snaith-Hamilton Pleasure Scale;

[*] missing data from 1 participant.

Table 2

Neural Activation During Reward Processing

Contrast	Voxels	X (mm)	Y (mm)	Z (mm)	$P_{FDR-corrected}$	Brain Region
Anticipation vs. Attainment	32665	−2	−54	−28	0.0010	Bilateral cerebellum anterior lobe, orbitofrontal cortex, middle frontal gyrus, anterior cingulate cortex, midcingulate cortex, posterior medial frontal cortex, precuneus, caudate, putamen, thalamus, insula, ventral striatum (nucleus accumbens), left hippocampus, left middle occipital gyrus
		−16	−20	60	0.0010	Left paracentral lobule
		−8	−70	50	0.0010	Left precuneus
		30	−28	48	0.0010	Right postcentral gyrus
		14	−42	48	0.0010	Right precuneus
		8	−64	48	0.0010	Right precuneus
		−50	−2	46	0.0010	Left precentral gyrus
	381	0	−56	24	0.0039	Bilateral precuneus/posterior cingulate cortex
		14	−44	8	0.0110	Right precuneus
		8	−44	16	0.0398	Right precuneus
	310	64	−40	24	0.0105	Right inferior parietal lobule (supramarginal gyrus)
		52	−56	24	0.0117	Right angular gyrus
		60	−54	24	0.0123	Right angular gyrus
		56	−58	26	0.0145	Right angular gyrus
		64	−48	18	0.0229	Right superior temporal gyrus
	201	62	−4	−20	0.0214	Right middle temporal gyrus

Contrast	Voxels	X (mm)	Y (mm)	Z (mm)	$p_{FDR\text{-}corrected}$	Brain Region
		54	−20	−10	0.0288	Right middle temporal gyrus
		54	−16	−14	0.0302	Right middle temporal gyrus
		48	0	−22	0.0302	Right middle temporal gyrus
		54	−2	−20	0.0324	Right middle temporal gyrus
		46	−26	−8	0.0339	Right middle temporal gyrus
	29	−42	22	26	0.0295	Left inferior frontal gyrus
		−36	18	24	0.0479	Left inferior frontal gyrus
	16	−22	−40	−4	0.0229	Left parahippocampal gyrus/hippocampus
	4	54	2	−30	0.0331	Right middle temporal gyrus
	3	16	54	2	0.0417	Right superior medial frontal gyrus
	2	−16	−102	−2	0.0324	Left cuneus
	1	−44	22	18	0.0490	Left inferior frontal gyrus
	1	−16	−14	−20	0.0417	Left hippocampus/parahippocampal gyrus
	1	54	−4	−30	0.0398	Right fusiform gyrus
	1	−8	−64	−32	0.0501	Left cerebellum anterior lobe
Attainment *vs.* Anticipation	16852	18	−36	−24	0.0043	Bilateral cerebellum anterior and posterior lobe, cuneus, lingual gyrus, hippocampus, parahippocampal gyrus, fusiform gyrus, precuneus, posterior cingulate cortex, middle and superior occipital gyrus, caudate, putamen, right inferior orbitofrontal cortex
		−20	−14	42	0.0043	Left caudate
		−18	2	40	0.0043	Left caudate

Contrast	Voxels	X (mm)	Y (mm)	Z (mm)	$p_{FDR\text{-}corrected}$	Brain Region
		30	0	34	0.0043	Right caudate
		−18	2	32	0.0043	Left caudate
		−22	−46	28	0.0043	Left parietal lobe
		22	−90	28	0.0043	Right cuneus
	203	46	0	−14	0.0043	Right superior temporal lobe/insula
	35	38	14	−22	0.0170	Right superior temporal pole
		42	10	−22	0.0182	Right superior temporal pole
	2	38	28	−16	0.0437	Right inferior orbitofrontal cortex
	1	48	−52	54	0.0501	Right inferior parietal lobule
	1	52	−56	44	0.0490	Right inferior parietal lobule
	1	−44	−4	−6	0.0479	Left insula
	1	−34	−80	−18	0.0479	Left fusiform gyrus
	1	−44	−12	−24	0.0447	Left inferior temporal gyrus
Positive Prediction Error	101216	−22	−74	−52	0.0010	Bilateral cerebellum posterior and anterior lobe, lingual gyrus, fusiform gyrus, cuneus, precuneus, inferior parietal lobule, insula, inferior temporal gyrus, middle temporal gyrus, superior temporal gyrus, middle frontal gyrus, inferior frontal gyrus, superior frontal gyrus, anterior cingulate cortex, midcingulate cortex, posterior cingulate cortex, parahippocampal gyrus, amygdala, thalamus, caudate, putamen, ventral striatum (nucleus accumbens), medial orbitofrontal cortex, hippocampus
		28	−42	70	0.0010	Right postcentral gyrus

Author Manuscript

Author Manuscript

Author Manuscript

Author Manuscript

Contrast	Voxels	X (mm)	Y (mm)	Z (mm)	$p_{FDR\text{-}corrected}$	Brain Region
		14	−6	68	0.0010	Right supplementary motor area
		6	16	64	0.0010	Right supplementary motor area
		30	6	64	0.0010	Right superior frontal gyrus
		14	6	60	0.0010	Right supplementary motor area
		18	10	58	0.0010	Right superior frontal gyrus
	7	50	−18	56	0.0457	Right postcentral gyrus
		50	−14	54	0.0490	Right postcentral gyrus
	2	−40	−58	46	0.0479	Left angular gyrus/inferior parietal lobule
	1	−18	−56	70	0.0490	Left superior parietal lobule
	1	−16	44	−8	0.0490	Left superior orbitofrontal cortex
	1	−38	40	−10	0.0437	Left inferior orbitofrontal cortex

Note. One-sample t-tests controlling for age examined group-level whole-brain activation for all contrasts of interest. Permutation testing with threshold-free cluster enhancement analyses, false discovery rate (FDR) corrected for multiple comparisons ($p < .05$). Coordinates are listed in MNI space.

Table 3

Correlations Between Reward Processing and Anhedonia

Contrast	Voxels	X (mm)	Y (mm)	Z (mm)	$p_{uncorrected}$	Region
SHAPS and Reward Anticipation (+ Correlation)	15	38	−54	36	0.00060	Right angular gyrus
SHAPS and Reward Attainment (+ Correlation)	None					
SHAPS and PPE (+ Correlation)	11	−32	−74	38	0.00030	Left precuneus/Brodmann area 19

Note. Correlations between brain activity during reward anticipation/attainment and anhedonia severity (SHAPS), controlling for age and depression severity (CDRS-R minus anhedonia item). Permutation testing with threshold-free cluster enhancement (TFCE) analyses, false discovery rate (FDR) corrected for multiple comparisons ($p < .05$) showed no significant results. No clusters survived the FDR correction. Exploratory results listed here are from the permutation testing with TFCE analyses, uncorrected ($p < 0.001$). Coordinates are listed in MNI space.